BIOCHEMICAL PHARMACOLOGY 73 (2007) 981–989

available at www.sciencedirect.com

ScienceDirect

journal homepage: www.elsevier.com/locate/biochempharm

Structure and function of eritadenine and its 3-deaza analogues: Potent inhibitors of S-adenosylhomocysteine hydrolase and hypocholesterolemic agents

Taro Yamada [a,1], *Junichi Komoto* [a,1], *Kaiyan Lou* [b], *Akiharu Ueki* [b], *Duy H. Hua* [b], *Kimio Sugiyama* [c], *Yoshimi Takata* [a,d], *Hirofumi Ogawa* [d], *Fusao Takusagawa* [a,*]

[a] *Department of Molecular Biosciences, University of Kansas, 1200 Sunnyside Avenue, Lawrence, KS 66045, USA*
[b] *Department of Chemistry, Kansas State University, 111 Willard Hall, Manhattan, KS 66506-3701, USA*
[c] *Department of Applied Biological Chemistry, Faculty of Agriculture, Shizuoka University, Shizuoka 422-8529, Japan*
[d] *Department of Molecular Neuroscience, Graduate School of Medicine, University of Toyama, 2630 Sugitani, Toyama 930-0194, Japan*

ARTICLE INFO

Article history:
Received 24 October 2006
Accepted 7 December 2006

Keywords:
Eritadenine
3-Deaza analogue
S-Adenosylhomocysteine hydrolase
Enzyme inhibition
Cholesterol reduction
Chemical synthesis

ABSTRACT

D-Eritadenine (DEA) is a potent inhibitor of S-adenosyl-L-homocysteine hydrolase (SAHH) and has hypocholesterolemic activity. We have hypothesized that 3-deaza-DEA (C3-DEA) and its analogues retain high level of SAHH inhibitory activity and have resistance to deamination and glycosidic bond hydrolysis *in vivo*. Such C3-DEA analogues would have much higher hypocholesterolemic activity. C3-DEA, and its methyl ester (C3-OMeDEA) and its methyl amido (C3-NMeDEA) were synthesized to examine their SAHH inhibitory and hypocholesterolemic activities. A crystal structure of SAHH containing C3-DEA was determined and confirmed that DEA and C3-DEA bound to the same site of SAHH with the same binding mode. The SAHH inhibitory activities of C3-DEA (K_I = 1.5 μM) and C3-OMeDEA (K_I = 1.5 μM) are significantly lower than that of DEA (K_I = 30 nM), while rats fed by C3-DEA and C3-OMeDEA decrease the total plasma cholesterol and phospholipids by 36–40% and 23%, respectively, which is similar to the level of reductions (42% and 27%) by DEA. C3-NMeDEA lost most of the SAHH inhibitory activity (K_I = 30 μM) and dietary C3-NMeDEA does not decrease cholesterol and phospholipid in plasma but decreases the triacylglycerol level by 16%. DEA and C3-DEA analogues are neither substrates nor inhibitors of adenosine deaminase.

* *Corresponding author*. Tel.: +1 785 864 4727; fax: +1 785 864 5321.
E-mail address: xraymain@ku.edu (F. Takusagawa).

[1] These authors contributed equally to this work.

Abbreviations: ADA, adenosine deaminase; Ado, adenosine; C3-Ado, 3-deaza-adenosine; C3-DEA, 3-deaza-DEA; C3-NMeDEA, 3-deaza-DEA methylamide; C3-OMeDEA, 3-deaza-DEA methylester; D244E[NADH + Ado*], NADH and 3′-keto-adenosine (Ado*) bound rat liver D244E mutated SAHH; Hcy, Homocysteine; DEA, D-eritadenine; NepA, neplanocin A; PC, phosphatidylcholine; PE, phosphatidylethanolamine; PEG, poly(ethylene glycol); rmsd, root-mean-square deviation; SAH, S-adenosyl-L-homocysteine; SAHH, S-adenosyl-L-homocysteine hydrolase; SAHH[NAD^+ + DEA], NAD^+ and DEA bound rat liver SAHH; SAHH[NAD^+ + C3-DEA], NAD^+ and C3-DEA bound rat liver SAHH; SAM, S-adenosyl-L-methionine

0006-2952/$ – see front matter
doi:10.1016/j.bcp.2006.12.014

1. Introduction

Hypercholesterolemia is now considered a major risk factor in the development of premature atherosclerosis. Several classes of hypolipidemic agents are now available for the control of hypercholesterolemia. These include the HMG-CoA reductase inhibitors [1] which inhibit cholesterol biosynthesis, the second generation fibric acid derivatives [2] which interfere with fatty acid synthesis and stimulates hepatic fatty acid oxidation, thus reducing the amount of fatty acid available to the liver for triglyceride synthesis, and the bile acid sequestrants [3] which interrupt the enterohepatic circulation of bile acids. The other types of hypocholesterolemic agents have also been developed. For example, the selective estrogen receptor modulators [4] which change lipid metabolism [5] and the potent inhibitors of acyl-CoAcholesterol acyltransferase [6–10] which inhibit cholesterol esterification.

Eritadenine [2(*R*),3(*R*)-dihydroxy-4-(9-adenyl)-butyric acid] (DEA) isolated from the *Lentinus edodes* mushroom (*Shiitake* in Japanese) has a hypocholesterolemic activity [11,12]. DEA is an acyclic sugar adenosine analogue shown in Scheme 1. Soon after discovery of the hypocholesterolemic activity, Okumura et al. synthesized more than 100 derivatives of DEA and evaluated the hypocholesterolemic activities of the compounds [13]. They have reported that the carboxyl function and atleast one hydroxyl group appear to be essential for activity. The most active derivatives were carboxylic acid esters with short-chain monohydroxy alcohols, which were 50 times more active than DEA and effective in lowering serum cholesterol of rats at the dose of 0.0001% in the diet. Since DEA is a potent *S*-adenosylhomocysteine hydrolase (SAHH) inhibitor [14], it has been postulated that dietary DEA inhibits the SAHH activity and increases the *S*-adenosylhomocysteine (SAH) level in liver, and consequently, the activities of *S*-adenosylmethionine (SAM)-dependent methyltransferases are decreased.

In addition to effects on phospholipid and fatty acid metabolism, DEA and its analogues (2*R*,3*R*)-dihydroxy-3-(9-adenyl)-propylic acid and 9-(2-phosphonylmethoxyethyl)adenine) have been found to be very potent inducers of mosaic spots on *Drosophia* wings in a dose-related fashion [15]. Also, DEA causes pronounced inhibition of intestinal phosphatases in the hemipteran insect *Pyrrhocoris apterus* [16].

Although DEA is a potent inhibitor of SAHH, *Shiitake*, which contains a relatively large amount (500–700 mg/kg) of DEA is not a poisonous mushroom. DEA is apparently degraded quickly in the liver. We have hypothesized that the hypocholesterolemic activity of DEA would increase if the degradation of DEA in the liver were slowed down [17]. The SAHH[NAD^+ + DEA] structure indicates that N3 of the adenine ring is not involved in H-bonding, and there is a relatively large space in front of N3 that is large enough to replace N3 with C–H [17]. Therefore, 3-deaza-DEA (C3-DEA) is expected to bind to the same active site and form the same H-bonds with SAHH as does DEA and to retain the same level of SAHH inhibitory activity. Since 3-deazaadenosine (C3-Ado) is resistant to glycosidic bond hydrolysis and 6-amino deamination [18,19], C3-DEA is expected to be degraded slowly in the liver. Consequently, C3-DEA would have a higher hypocholesterolemic activity than does DEA.

In order to improve the hypocholesterolemic activity of DEA, we have synthesized C3-DEA and its methylester (C3-OMeDEA) and methylamide (C3-NMeDEA) derivatives, measured the SAHH inhibitory activities and the hypocholesterolemic activities of the DEA analogues, and determined a crystal structure of SAHH containing C3-DEA.

2. Materials and methods

2.1. Chemical synthesis of 3-deaza-DEA analogues

3-Deaza-adenine was prepared from 4-chloroimidazo[4,5-c]pyridine [20] with hydrazine followed by W2 Raney nickel [21]. C3-DEA was prepared by following a method reported by Okumura et al. [22], in which 3-deaza-adenine was treated with sodium carbonate and (2*R*,3*R*)-cyclohexylidenedioxybutyrolactone in *N*,*N*-dimethylformamide (DMF). Acidic hydrolysis of the resulting protected C3-DEA with 4 M HCl in dioxane and water gave C3-DEA. Treatment of the above cyclohexylidene protected C3-DEA with a catalytic amount of concentrated sulfuric acid in methanol at 60 °C for 24 h provided C3-OMeDEA in excellent yield. C3-NMeDEA was synthesized by heating of C3-OMeDEA with methylamine in tetrahydrofuran (THF) and methanol in a sealed tube at 90 °C for 24 h.

2.1.1. (2*R*,3*R*)-4-(3-Deazaadenin-9-yl)-2,3-dihydroxybutanoic acid (C3-DEA) [23]

A solution of 0.81 g (6.0 mmol) of 3-deazaadenine, 1.78 g (9.0 mmol) of (2*R*,3*R*)-cyclohexylidenedioxybutyrolactone, and 0.64 g (6.0 mmol) of anhydrous sodium carbonate in 22 mL of DMF (distilled over CaH_2) was heated under reflux (bath temperature: 165 °C) for 15 h under argon. The resulting

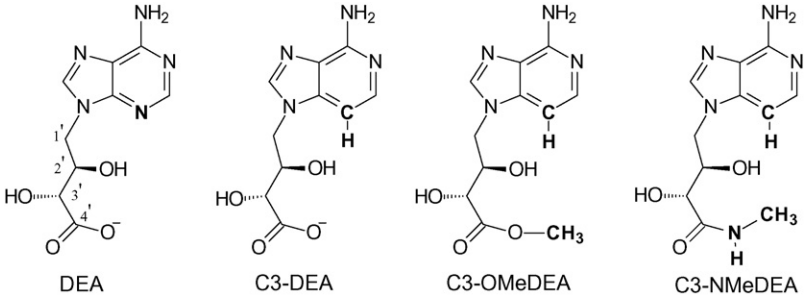

Scheme 1 – Chemical structures of DEA and C3-DEA analogues.

brown reaction mixture was cooled to 25 °C, neutralized with 0.72 g (12 mmol) of acetic acid, and DMF was removed by vacuum distillation. The residue was purified through silica gel column chromatography using a gradient mixture of dichloromethane and methanol as eluants to give 1.41 g (71% yield) of (2*R*,3*R*)-2,3-cyclohexylidenedioxy-4-(3-deazaadenin-9-yl)butanoic acid. $[\alpha]_D^{25} = +78$ (c 0.00048, CH_3OH); ^1H NMR [D_2O δ (ppm) from HOD as an internal standard]: 8.17 (s, 1H, NCHN), 7.73 (d, J = 6.4 Hz, 1H, CHN), 7.10 (d, J = 6.4 Hz, 1H, CH═), 4.74 (m, 2H, CHO), 4.37 (dd, J = 14, 1 Hz, 1H, CH_2), 4.20 (dd, J = 14, 10 Hz, 1H, CH_2), 1.9–1.3 (a series of m, 10H); ^{13}C NMR [D_2O δ (ppm) from CH_3OH as an internal standard]: 161.9, 137.9, 134.2, 131.8, 127.3, 124.7, 99.4, 86.7, 64.1, 61.8, 34.3, 24.3, 21.4, 11.8, 11.1, 10.6. MS (electrospray ionization) m/z 333.062 (M + 1; M^+, $C_{16}H_{20}N_4O_4$: 332.15).

A solution of 0.45 g (1.36 mmol) of (2*R*,3*R*)-2,3-cyclohexylidenedioxy-4-(3-deazaadenin-9-yl)butanoic acid and 3.4 mL of hydrochloric acid (4 M in dioxane) in 3 mL of water was stirred at 25 °C for 2 h. The solution was concentrated to dryness under vacuum to give 0.47 g of C3-DEA as a HCl salt. The compound was crystallized from water to give 0.25 g of pure C3-DEA·HCl [23]. $[\alpha]_D^{25} = +31$ (c 0.00045, H_2O); ^1H NMR [D_2O δ (ppm) from HOD as an internal standard]: 8.33 (s, 1H, NCHN), 7.65 (d, J = 7 Hz, 1H, CHN), 7.20 (d, J = 7 Hz, 1H, CH═), 4.50 (m, 2H), 4.32 (m, 2H); ^{13}C NMR [D_2O δ (ppm) from CH_3OH as an internal standard]: 175.2, 148.6, 146.6, 141.5, 129.8, 125.8, 100.1, 72.4, 71.5, 49.5. MS (electrospray ionization) m/z 252.929 (M + 1; M^+, $C_{10}H_{12}N_4O_4$).

2.1.2. (2*R*,3*R*)-Methyl 4-(3-deazaadenin-9-yl)-2,3-dihydroxybutanoate (C3-OMeDEA)

A solution of 0.383 g (1.15 mmol) of (2*R*,3*R*)-2,3-cyclohexylidenedioxy-4-(3-deazaadenin-9-yl)butanoic acid and 80 μL of concentrate H_2SO_4 in 15 mL of methanol was stirred at 60 °C for 24 h. The solution was neutralized with aqueous NH_4OH, concentrated to dryness, and crystallized from water to give 0.278 g (91% yield) of pure C3-OMeDEA. $[\alpha]_D^{25} = +6.0$ (c 0.001, CH_3OH); ^1H NMR [D_2O δ (ppm) from HOD as an internal standard]: 8.19 (s, 1H, NCHN), 7.70 (d, J = 7 Hz, 1H, CHN), 7.11 (d, J = 7 Hz, 1H, CH═), 4.46 (m, 2H), 4.34 (m, 2H), 3.65 (s, 3H, OMe); ^{13}C NMR [D_2O δ (ppm) from CH_3OH as an internal standard]: 167.0, 144.9, 143.5, 138.9, 134.0, 127.3, 92.9, 65.6, 64.4, 46.4, 40.5. MS (electrospray ionization) m/z 266.027 (M^+, $C_{11}H_{14}N_4O_4$). Anal. calcd. for $C_{11}H_{14}N_4O_4$: C, 49.62; H, 5.30. Found: C, 49.31; H, 5.59.

2.1.3. (2*R*,3*R*)-*N*-Methyl-4-(3-deazaadenin-9-yl)-2,3-dihydroxybutanamide (C3-NMeDEA)

A solution of 0.37 g (1.39 mmol) of C3-OMeDEA in 1.5 mL of methanol and 5 mL of methylamine (2 M solution in THF) was heated in a sealed tube at 90 °C for 24 h. The solution was cooled, concentrated to dryness, and column chromatographed on silica gel using methanol:dichloromethane (2:3) as an eluant to give 0.305 g (83% yield) of C3-NMeDEA. $[\alpha]_D^{25} = +15$ (c 0.0006, CH_3OH); ^1H NMR [D_2O δ (ppm) from HOD as an internal standard]: 8.12 (s, 1H, NCHN), 7.76 (d, J = 6.4 Hz, 1H, CHN), 7.02 (d, J = 6.4 Hz, 1H, CH═), 4.45–4.26 (m, 4H), 2.57 (s, 3H, NMe). ^{13}C NMR [D_2O δ (ppm) from CH_3OH as an internal standard]: 166.9, 145.4, 144.5, 142.0, 132.0, 125.0, 84.1, 62.5, 61.7, 44.7, 33.0. MS (electrospray ionization) m/z 266.00 (M + 1; M^+, $C_{11}H_{15}N_5O_3$). Anal. calcd. for $C_{11}H_{15}N_5O_3$: C, 49.81; H, 5.70. Found: C, 48.93; H, 6.01.

2.2. Purification of SAHH

SAHH used in this study is the recombinant rat liver enzyme produced in *Escherichia coli* JM109 transformed with a pUC118 plasmid that contains the coding sequence of rat SAHH cDNA [24]. The enzyme was purified to homogeneity from *E. coli* extracts by gel filtration over Sephacryl S-300 and DEAE-cellulose chromatography as described previously [24].

2.3. SAHH inhibitory activities

SAHH catalyzes SAH hydrolysis to Ado and Hcy, and Ado is quickly converted to inosine in the presence of adenosine deaminase (ADA). Since absorptions of the adenine and hypoxanthine rings are significantly different at 265 nm, we can measure the SAH hydrolysis rate of SAHH in the presence of the inhibitors spectrophotometrically in the presence of excess ADA by measuring the rate of appearance of inosine [25]. A 5 μL aliquot of the protein solution (1.0 mg/mL concentration) was added to 995 μL of the assay mixture containing known concentrations of SAH, inhibitor, and 1.4 units of calf intestine ADA (Sigma, MO, USA) in 50 mM potassium phosphate (pH 7.2), and the decrease of absorbance at 265 nm due to the conversion of the product Ado to inosine was followed continuously at 22 °C. The same experiment was repeated five times with different SAH concentrations (10, 15, 20, 30, and 50 μM). The inhibitor concentrations were 0, 10, 20, 30, 40 nM for DEA, 0, 0.5, 1.0, 1.5, 2.0 μM for C3-DEA and C3-OMeDEA, and 0, 25, 50, 75 μM for C3-NMeDEA. The initial velocities (v_0) at known inhibitor and substrate concentration were calculated from the slope of ΔA and $\Delta\varepsilon = 8.1 \times 10^3\ M^{-1}\ cm^{-1}$. From a Lineweaver–Burk plot (1/[SAH] versus $1/v_0$), the slope at a known inhibitor concentration was determined by least-square fitting (Fig. 1). All lines by various inhibitor concentrations intersect at one point within experimental error. However, the intersection points are not on the $1/v_0$ axis (see details in Section 3). The K_I value of each inhibitor was determined from a plot of the inhibitor concentration versus slope of Lineweaver–Burk plot using the following relation:

$$\text{slope} = \left(\frac{K_M}{V_{max}K_I}\right)[I] + \frac{K_M}{V_{max}}$$

2.4. Adenosine deaminase (ADA) inhibitory activities

ADA from calf intestine was purchased from Sigma and used without further purification. The ADA inhibitory activities of DEA and C3-DEA analogues were measured by the same procedure applied for the SAHH inhibitory assay. In this case, adenosine (Ado) is the substrate and DEA or C3-DEA analogues are inhibitors. The rate of appearance of inosine from Ado was measured by the decrease of absorbance at 265 nm. The slope of ΔA was not changed with various concentrations of DEA or C3-DEA analogues (0.0–50 μM), indicating that DEA and C3-DEA analogues do not have an ADA inhibitory activity.

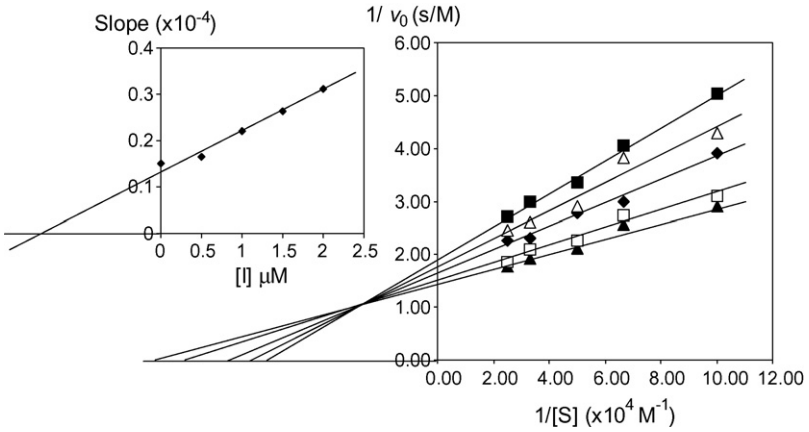

Fig. 1 – Inhibition of SAHH by C3-OMeDEA. Inhibitor concentrations were 0 μM (▲), 0.5 μM (□), 1.0 μM (◆), 1.5 μM (△) or 2.0 μM (■). Inset: plot of the slope of the lines as a function of [I]. The initial velocity v_0 was converted to mol/s with 1 mol of SAHH, so that K_M and k_{cat} can be determined from the data in the absence of inhibitor (▲) (y-axis intercept = $1/V_{max}$ = 1.4 s/mol and slope = $K_M/V_{max} = 1.51 \times 10^{-5}$ M s/mol. From these values, $K_M = 1.51 \times 10^{-5}/1.4 = 10.8$ μM and $k_{cat} = V_{max}/[E] = 1/1.4 = 0.71\ s^{-1}$). It is noted that the Lineweaver–Burk plots of DEA, C3-DEA, C3-NMeDEA are quite similar to that of C3-OMeDEA.

The deamination rates of DEA and C3-DEA analogues by ADA were also measured by the same procedure described above. No decrease of absorbance at 265 nm was observed, indicating that DEA and C3-DEA analogues are not deaminated by ADA.

2.5. Animals and diets

Fifty male 6-week-old rats of the Wistar strain ($n = 50$), weighing 125–135 g, were received from Japan SLC (Hamamatsu, Japan). The rats were individually housed in hanging stainless wire cages kept in an isolated room at a controlled temperature of 23–25 °C and humidity of 40–60%. Lights were maintained on a 12-h cycle (lights on from 6:00 to 18:00 h.). Rats were divided into five groups ($n = 10$) with similar mean body weights (129 g) and allowed free access to the experimental diets and water for 14 days. In the present study, five experimental diets were used: a control diet, a diet supplemented with DEA at a level of 50 mg/kg, a diet supplemented with C3-DEA at a level of 50 mg/kg, a diet supplemented with C3-OMeDEA at a level of 50 mg/kg, and a diet supplemented with C3-NMeDEA at a level of 50 mg/kg. The composition of the control diet was as follows (g/kg): casein, 250; cornstarch, 429; sucrose, 200; corn oil, 50; AIN-93 mineral mixture [26], 35; AIN-93 vitamin mixture [26], 10; choline bitartrate, 5; cellulose, 20; lactose, 1. DEA and DEA analogues were mixed with lactose and added to the diet.

2.6. Lipid analysis

At the end of the 14 days feeding period, rats that had not been deprived of food were decapitated between 12:00 and 12:30 h. Plasma was separated from the heparinized whole blood by centrifugation at 2000 × *g* for 20 min at 4 °C and stored at −180 °C until analyses for plasma lipid concentrations. The plasma concentrations of the total cholesterol (VLDL + LDL + HDL), triglycerols, and phospholipids were measured enzymatically with kits (cholesterol E-test, triglyceride E-test and phospholipid B-test, respectively; Wako Pure Chemical, Osaka, Japan). The results are listed in Table 1.

2.7. Crystal structure determination of SAHH[NAD$^+$ + C3-DEA]

A batch method was employed for crystallization of the enzyme. All crystallization experiments were conducted at

Table 1 – Effects of dietary supplementation with DEA or C3-DEA analogues on plasma lipid concentrations in rats[a]

	Plasma lipids (mmol/L)		
	Total cholesterol	Triacylglycerols	Phospholipids
Control	2.31 ± 0.03 a	1.45 ± 0.08 ab	2.28 ± 0.06 a
Control + DEA	1.34 ± 0.07 b	1.52 ± 0.06 a	1.67 ± 0.06 b
Control + C3-DEA	1.38 ± 0.05 b	1.45 ± 0.11 ab	1.75 ± 0.02 b
Control + C3-OMeDEA	1.47 ± 0.02 b	1.53 ± 0.08 a	1.75 ± 0.06 b
Control + C3-NMeDEA	2.30 ± 0.04 a	1.22 ± 0.05 b	2.28 ± 0.04 a

[a] Values are mean ± S.E.M., $n = 10$. Treatment effects (DEA and C3-DEA analogue supplementation) were analyzed by ANOVA, and the differences between means were tested using Duncan's multiple range test [39]. A P value of 0.05 or less was considered significant. Values in each column with letter (a) are significantly different from those with the letter (b), while values with the letters (ab) are not significantly different from those with either the letters (a) or (b).

22 °C. Small crystals of the enzyme were grown in a solution containing 2 mM C3-DEA, 15% (w/v) PEG 8000, 50 mM MES buffer pH 6.5, and 2% (v/v) glycerol with a protein concentration of 2 mg/mL. The plate-shape crystals suitable for X-ray diffraction were grown for 2 weeks.

A crystal having dimensions ~0.3 mm × 0.2 mm × 0.1 mm in a drop was scooped out with a nylon loop and was dipped into a cryoprotectant solution containing 18% ethylene glycol, 15% (w/v) PEG 8000, 50 mM MES buffer pH 6.5, and 2% (v/v) glycerol for 30 s before it was frozen in liquid nitrogen. The frozen crystal was transferred onto a Rigaku RAXIS IIc imaging plate X-ray diffractometer with a rotating anode X-ray generator as an X-ray source (Cu Kα radiation operated at 50 kV and 100 mA). The diffraction data were measured up to 2.8 Å resolution at −180 °C. The data were processed with the program DENZO and SCALEPACK [27].

The unit cell dimensions and the assigned space group indicated the crystal of SAHH[NAD^+ + C3-DEA] is isomorphous to that of SAHH[NAD^+ + DEA] [17], and two tetrameric enzymes (eight subunits) are in the asymmetric unit. The crystal structure was refined by a standard refinement procedure in the X-PLOR protocol with the non-crystallographic symmetry restraint [28]. During the later stages of refinement, difference maps ($F_o - F_c$ maps) showed a large significant residual electron density peak in the region of the active site of each subunit. The shape of the electron-density peak suggested that each individual subunit contains C3-DEA, and a C3-DEA molecule was fit into each electron density peak (Fig. 2). During the final refinement stage, well-defined residual electron density peaks in difference maps were assigned to water molecules if peaks were able to bind the protein molecules with hydrogen bonds.

The crystallographic refinement parameters (Table 2), final ($2F_o - F_c$) maps, and conformational analysis by PROCHECK [29] indicate that the crystal structure of SAHH[NAD^+ + C3-DEA] has been determined with acceptable statistics. Since the eight subunits are identical at a resolution of 2.8 Å, they have been tightly restrained to have the same structure (rmsd ≤ 0.05 Å) in order to increase the quality of the structure. The atomic coordinates have been deposited in the Protein Data Bank (Entry name: 2H5L).

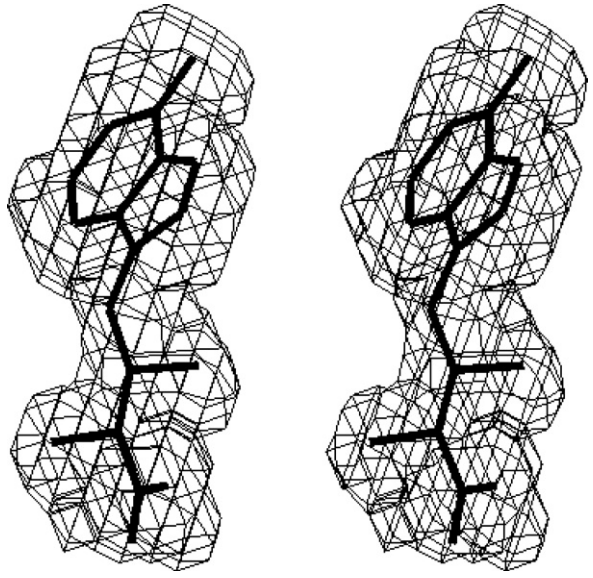

Fig. 2 – A ($2F_o - F_c$) map showing electron density peak of C3-DEA at the contour level of 1.2σ.

Table 2 – Experimental details and refinement parameters of crystal structure analyses

Experimental details	
Resolution (Å)	10.0–2.8
Number of crystals	1
Number of reflections measured	226,127
Number of unique reflections[a]	78,969
% complete	91.8
R_{sym}[b]	0.157
$I/\sigma(I)$[c]	3.8
Refinement parameters	
Number of residues	3,448
Number of NAD^+ molecules	8
Number of C3-DEA molecules	8
Number of water molecules	291
R[d]	0.245
Free R	0.284
rmsd from the ideal values	
Bond (Å)	0.007
Angle (°)	1.12
Torsion angle (°)	25.8
Luzzati coordinated errors (Å)	0.034
Ramachandran plot	
Residues in most favored region (%)	89.6
Residues in additional allowed region (%)	10.4

Space group: $P2_1$; cell dimension (Å): a = 90.50, b = 178.60, c = 112.66, β = 107.9°; M_r of subunit: 47,000; number of subunits in the unit cell: 16; V_M = 2.30 Å^3; percentage of solvent content: 47%.

[a] Unique reflections in the range between 10.0 Å and highest resolution.

[b] $R_{sym} = \sum_h \sum_i |I_{hi} - \langle I_h \rangle| / \sum_h \sum_i |I_{hi}|$.

[c] $I/\sigma(I)$ in 2.9–2.8 Å resolution range.

[d] $R_{cryst} = \sum_h |F_o - F_c| / \sum_h |F_o|$.

3. Results and discussion

3.1. SAHH and ADA inhibitory activities of DEA analogues

The enzyme activity of recombinant rat liver SAHH was measured in the hydrolytic direction spectrophotometrically [25]. The K_M for SAH hydrolysis was determined to be 10.7 μM and the k_{cat} was 0.71 s^{-1} (see Fig. 1). Several K_M and k_{cat} values of the recombinant rat liver SAHH have been reported: K_M = 14.1 μM and k_{cat} = 0.81 s^{-1} [30], K_M = 9.7 μM and k_{cat} = 0.86 s^{-1} [31], and K_M = 8.8 μM and k_{cat} = 1.0 s^{-1} [32]. Thus, the values we obtained are consistent with values reported previously.

The K_I value (30 ± 0.3 nM) of DEA obtained in this study indicates that DEA is a potent inhibitor of SAHH. The K_I value (1.5 ± 0.2 μM) of C3-DEA is significantly increased from that of DEA, indicating that modification of adenine to 3-deazaadenine reduces the inhibitory activities of the analogues. Conversion of the carboxylic group to a methylester (C3-OMeDEA) does not alter the inhibitory activity but modification of the carboxyl group to methylamide (C3-NMeDEA)

reduces the inhibitory activity significantly (K_I increases from 1.5 ± 0.2 μM to 30 ± 0.5 μM). DEA and C3-DEA analogues were found to be neither inhibitors nor substrates of ADA.

As shown below, DEA and C3-DEA analogues compete with the substrate for the binding site and thus are competitive inhibitors. However, as shown in Fig. 1, Lineweaver–Burk plots indicate that DEA and C3-DEA analogues are mixed inhibitors. In this case, the enzyme forms two complexes, EI (enzyme–inhibitor) and ESI (enzyme–substrate–inhibitor), and the ESI is a non-reactive complex. The crystal structures of SAHH show that SAHH has two distinct conformations (E_{op} (opened conformation) and E_{cl} (closed conformation)) [32–34]. Substrate/inhibitor can only bind to or dissociate from E_{op}, while the substrate/inhibitor bound enzyme has two conformations (E_{op} and E_{cl}). For the DEA and C3-DEA analogue cases, there are two different EI complexes ($E_{op}I$ and $E_{cl}I$). Since inhibitor I cannot dissociate from the $E_{cl}I$ complex, the $E_{cl}I$ is a non-reactive complex similar to the ESI complex. Therefore, the lines of Lineweaver–Burk plots are no longer intersected on the $1/v_0$ axis as like a simple competitive inhibitor, but the Lineweaver–Burk plots look like a mixed inhibitor. Similar Lineweaver–Burk plot of a competitive inhibitor of SAHH has been reported [31].

3.2. *Crystal structure of SAHH[NAD⁺ + C3-DEA]*

The crystal contains two crystallographically independent tetrameric SAHH molecules, with each subunit of the tetrameric SAHH molecule related by 222 symmetry (Fig. 3A). The eight independent subunits are identical at a

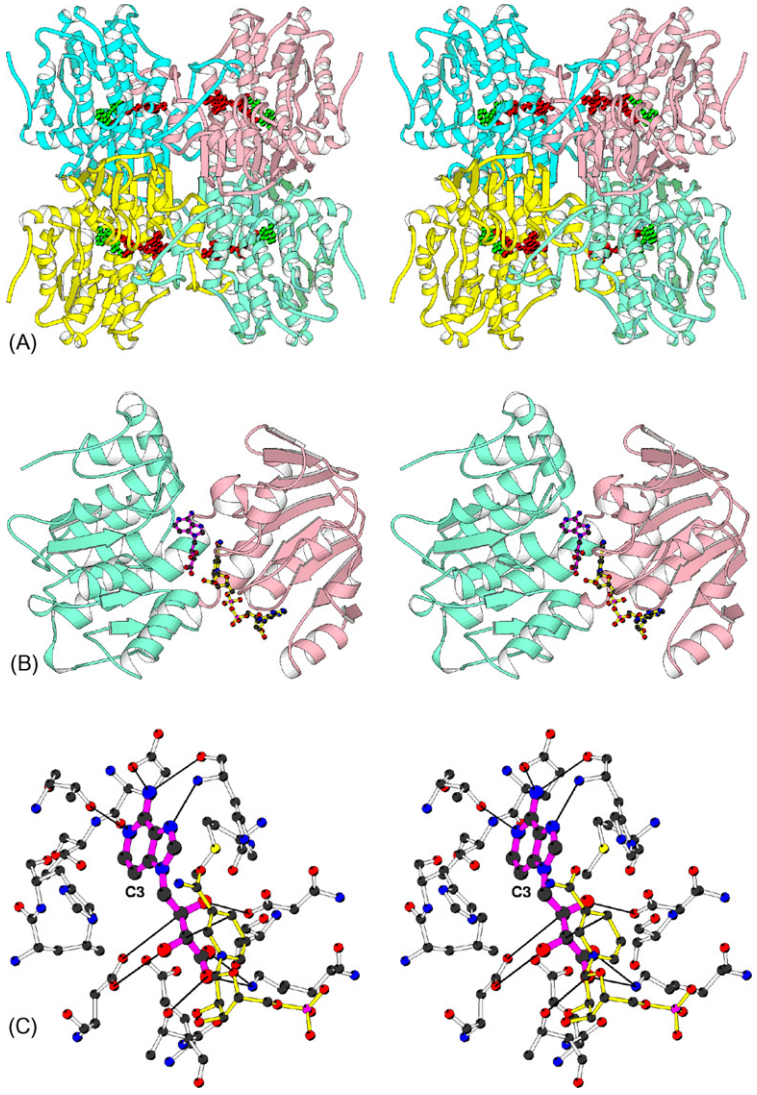

Fig. 3 – (A) Tetrameric structure of SAHH. Subunits related by a pseudo 222 symmetry are cyan, light-pink, aquamarine, and yellow, respectively. Four tightly bound NAD⁺ molecules and four C3-DEA are illustrated as red and green balls, respectively. (B) Ribbon drawing of a single subunit of SAHH[NAD⁺ + C3-DEA] showing catalytic (aquamarine) and NAD-binding (light-pink) domains. The bound NAD⁺ and C3-DEA are illustrated by ball-and-stick modes. The C-terminal domain is omitted for clarity. (C) A C3-DEA molecule in the active site. Possible hydrogen bonds (<3.5 Å) between C3-DEA and SAHH are illustrated by thin lines (see details in Fig. 4A). (For interpretation of the references to color in this figure legend, the reader is referred to the web version of the article.)

resolution of 2.8 Å (rmsd ≤ 0.05 Å). The structure of SAHH[NAD$^+$ + C3-DEA] is isomorphous to that found in SAHH[NAD$^+$ + DEA] [17]. The rmsd between the two SAHH structures is 0.56 Å, indicating that the 3D-structures of SAHH in SAHH[NAD$^+$ + DEA] and SAHH[NAD$^+$ + C3-DEA] are the same within experimental error. As shown in Fig. 3B, NAD$^+$ and C3-DEA bind to the NAD-binding domain and the catalytic domain, respectively. SAHH has two distinct conformations, opened and closed, by rotating the catalytic domain ~18° around the molecular hinge section [32–34]. The SAHH in SAHH[NAD$^+$ + C3-DEA] has a closed conformation, and the bound C3-DEA and NAD$^+$ are completely buried between the catalytic and NAD-binding domains, indicating that C3-DEA cannot bind to or dissociate from SAHH in the closed conformation.

As predicted [17], C3-DEA binds to the same site of SAHH as DEA and the 3-deaza-adenine ring of C3-DEA fits well in the adenine-ring binding-site of DEA without short contacts (Fig. 3C). The structure of SAHH in SAHH[NAD$^+$ + C3-DEA] is remarkably similar to that of the NADH-bound enzyme D244E[NADH + Ado*] [34], indicating that the oxidation state of NAD does not affect the conformation of SAHH. Furthermore, the geometry of the substrate-binding site is not changed by binding quite differently shaped molecules (Ado versus C3-DEA), indicating that the substrate-binding site is relatively rigid.

The structures of SAHH[NAD$^+$ + DEA] and SAHH[NAD$^+$ + C3-DEA] suggest why DEA is a potent competitive inhibitor (K_I = 30 nM). DEA is an acyclic sugar Ado analogue, and the two chiral centers (C2′ and C3′) have chirality opposite to those of Ado and cyclic sugar Ado analogues. Nevertheless, DEA fits well in the Ado binding site of SAHH and forms similar H-bonds with SAHH as seen in D244E[NADH + Ado*], suggesting that DEA is quite flexible. Indeed, DEA in the sodium salt crystal structure has a bent conformation (torsion angle C1′–C2′–C3′–C4′ = −60°), while DEA in the SAHH complex has an extended conformation (torsion angles C1′–C2′–C3′–C4′ = 180°) [17]. Obviously, the bent DEA does not fit in the relatively rigid active site of SAHH. In comparison to Ado in D244E[NADH + Ado*], DEA can be involved in more H-bonding since DEA has more H-bond forming oxygens than Ado (Fig. 4). Furthermore, the carboxylate group of DEA forms a salt linkage with the ammonia group (N_Z) of K185, which is not seen in D244E[NADH + Ado*]. In the proposed catalytic mechanism [32], the bound NAD$^+$ abstracts the H3′ hydrogen, and the carboxylate of D130 removes the H4′ proton of Ado, and the intermediate, 3′-keto-4′,5′-dehydroadenosine is produced. As shown in Fig. 3C, the hypothetical H3′ and H4′ of Ado in D244E[NADH + Ado*] are pointed toward C4 of NAD and O_D of D130, respectively, and the [Ado*]C3′···C4[NAD] and [Ado*]C4′···O_D[D130] distances are less than 3.5 Å, suggesting that there are significant interactions which induce the catalytic reaction. Similar interactions ([DEA]C3′···C4[NAD] and [DEA]C2′···O_D[D130]) are observed in SAHH[NAD$^+$ + DEA] although DEA is not oxidized by the bound NAD$^+$. Once the catalytic reaction occurs (i.e. Ado is converted to 3′-keto-4′,5′-dehydroadenosine), only the O2′ and O3′ of Ado can participate in H-bonding with SAHH, and thus the affinity of 3′-keto-4′,5′-dehydroadenosine is decreased and stability of the closed conformation is decreased, whereas all four oxygens (O2′, O3′, O4a′, and O4b′) of the intact DEA are involved in hydrogen bonding in the closed conformation. Therefore, it appears that DEA binds to SAHH more tightly than the substrate Ado does, and consequently, the dissociation constant K_I becomes small.

3.3. *Modification effects on the SAHH inhibitory activity*

The SAHH inhibitory activity of C3-DEA (K_I = 1.5 μM) is significantly decreased from that of DEA (K_I = 30 nM). Since the crystal structures of SAHH[NAD$^+$ + DEA] and SAHH[NAD$^+$ + C3-DEA] indicate that the binding schemes of DEA and C3-DEA to the active site of SAHH are the same, the N3 to C3 adenine ring modification apparently reduces the affinity of C3-DEA to the active site of SAHH. Although the crystal structure of SAHH[NAD$^+$ + DEA] which has a closed conformation does not show a water between N3 of the adenine ring and the protein, the inhibition data of DEA and C3-DEA indicate that a water is most likely coordinated on N3 when DEA binds to SAHH with the opened conformation. The bound water would increase the initial binding affinity of DEA to SAHH with an opened conformation and would be released (or disordered) when SAHH has a closed conformation.

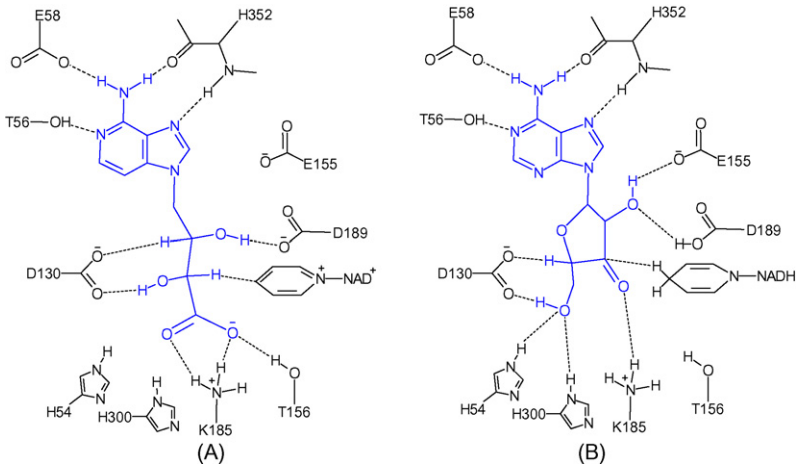

Fig. 4 – Schematic diagrams of interactions of C3-DEA and Ado* in the active site. (A) C3-DEA in SAHH[NAD$^+$ + C3-DEA], and (B) Ado* in D244E[NADH + Ado*]. Dashed lines indicate the possible hydrogen bonds and interactions.

In the structure of SAHH[NAD^+ + C3-DEA], there are relatively large spaces around the carboxyl oxygens that are large enough to accommodate a methyl group. Although the charge interaction between the negatively charged carboxylate group and the positively charged ammonia group of K185 is no longer available, C3-OMeDEA can bind to the same site of SAHH and form the same H-bonding as in SAHH[NAD^+ + C3-DEA]. Indeed, the SAHH inhibitory activity of C3-DEA (K_I = 1.5 μM) and C3-OMeDEA (K_I = 1.5 μM) are equal.

On the other hand, the SAHH inhibitory activity of C3-NMeDEA is significantly reduced (K_I = 30 μM). In the crystal structures of SAHH[NAD^+ + DEA] and SAHH[NAD^+ + C3-DEA], the H-bond acceptor carboxylate group of DEA or C3-DEA form two H-bonds with the H-bond donor ammonia group (N_Z) of K185. The methylamide group of C3-NMeDEA cannot form a H-bond with the ammonia group of K185 because both groups are H-bond donors. Furthermore, the methylamide group would have an unfavorable charge interaction with the ammonia group. Therefore, the reduction of SAHH inhibitory activity of C3-NMeDEA compared to C3-DEA is due to disruption of the salt-linkage between the carboxyl and ammonia groups.

It is believed that most of DEA is quickly degraded in the rat intestine and liver. In general, degradation of adenosine derivatives occurs initially by deamination of N6 by adenosine deaminase (ADA), followed by the glycosidic bond cleavage by purine nucleoside phosphorylase. Since the crystal structure of ADA containing an adenosine transition analogue indicates that N3 of the adenine ring participates in H-bonding with the amide group of G184 [35], C3-adenosine analogues are expected to be degraded much slower than adenosine analogues. Indeed, Ado is the substrate of ADA, but C3-Ado is a weak inhibitor of ADA (K_I = 400 μM) [19]. Therefore, C3-DEA is expected not to bind to ADA and not be degraded by ADA, while C3-DEA can bind to and inhibit SAHH. For this reason we synthesized the C3-DEA analogues. Surprisingly, both DEA and C3-DEA analogues are found to be neither a substrate nor an inhibitor of ADA. A reexamination of the model structure suggests that a DEA molecule fits well in the Ado binding site of the ADA structure, but the negatively charged carboxyl groups of DEA would have an unfavorable charge interaction with D19. This interaction might prevent DEA from binding to the ADA active site.

3.4. *Why does the 3-deaza-modification not alter the SAHH inhibitory activity of mechanism-based inhibitors?*

Interestingly, a mechanism-based SAHH inhibitor neplanocin A (NepA) and its 3-deaza-neplanocin A (C3-NepA) are reported to have the same levels of inhibitory activities (K_I = 7 nM versus 23 nM) [36]. In the crystal structures of SAHH[-NAD^+ + C3-DEA], SAHH[NAD^+ + DEA], and SAHH[NADH + -NepA] [37], C3-DEA, DEA, and NepA bind to the same site of SAHH and their adenine rings form the same H-bond networks. Therefore, why does the C3-DEA modification decrease the SAHH inhibitory but the C3-NepA modification does not? The sugar moiety of NepA is oxidized by the bound NAD^+ in the SAHH active site. The inhibitory mechanism of NepA involves NepA reducing the tightly bound NAD^+ to NADH and becoming an irreversible oxidized NepA which stabilizes the closed conformation of SAHH. Therefore, the irreversible oxidation reaction is the major inhibitory power for NepA. On the other hand, the sugar moiety of DEA is not oxidized by the bound NAD^+, and thus, the SAHH inhibitor activity of DEA is due to tight binding to the active site of SAHH. The weak binding of the 3-deaza-adenine ring reduces the affinity of C3-DEA for SAHH, and consequently, the C3-DEA analogues have decreased SAHH inhibitory activity.

3.5. *Effects on the lipid concentrations in plasma by DEA and C3-DEA analogues*

Dietary DEA and C3-DEA analogues did not affect the growth and food consumption of rats. Dietary DEA, C3-DEA, and C3-OMeDEA did significantly decrease the plasma concentrations of cholesterol (VLDL + LDL + HDL) and phospholipids (Table 1). However, dietary C3-NMeDEA did not affect the plasma concentrations of the total cholesterol and phospholipids. The plasma concentration of triacylglycerol was significantly decreased by dietary C3-NMeDEA, but not by DEA, C3-DEA, and C3-OMeDEA. These observations suggest that C3-DEA and C3-OMeDEA have the same biological activity as DEA, but the methylamide modification (C3-NMeDEA) might alter the molecule to make it bind to different targets and thus show different biological activities.

There is a strong correlation between cholesterol and phospholipid concentrations. In the control and the C3-NMeDEA fed rats, the ratio of the cholesterol and phospholipid concentrations is near 1.0, while those ratios in the DEA, C3-DEA, and C3-OMeDEA fed rats are reduced to 0.8, suggesting that DEA, C3-DEA, and C3-OMeDEA decrease the concentration of higher density lipoproteins such as LDL and HDL in plasma. Indeed, DEA decreases the LDL and HDL concentration in plasma but not the VLDL concentration [38]. These observations suggest that DEA, C3-DEA, and C3-OMeDEA stimulate tissues, especially liver tissue to take up plasma lipoprotein cholesterol and phospholipids from higher density lipoproteins.

Acknowledgements

We wish to express our thanks to Professor Richard H. Himes for a critical reading of this manuscript and valuable comments. This work was supported by American Heart Association grant 0455454Z to FT.

REFERENCES

[1] Illingworth DR, Tobert JA. A review of clinical trials comparing HMG-CoA reductase inhibitors. Clin Ther 1994;16:366–85.
[2] Sirtori CR, Franceschini G. Effects of fibrates on serum lipids and atherosclerosis. Pharmacol Ther 1988;37:167–91.
[3] Einarsson R, Ericsson S, Ewerth S, Reihner E, Rudling M, Stahlberg D, et al. Bile acid sequestrants: mechanisms of action on bile acid and cholesterol metabolism. Eur J Clin Pharmacol 1991;40:S53–8.
[4] Doshida M, Ohmichi M, Tsutsumi S, Kawagoe J, Takahashi T, Du B, et al. Raloxifene increases proliferation and

upregulates telomerase activity in human umbilical vein endothelial cells. J Biol Chem 2006;281:24270–8.
[5] Walsh BW, Kuller LH, Wild RA, Paul S, Farmer M, Lawrence JB, et al. Effects of raloxifene on serum lipids and coagulation factors in healthy postmenopausal women. JAMA 1998;279:1445–51.
[6] Matsuda K. ACAT inhibitors as antiatherosclerotic agents: compounds and mechanisms. Med Res Rev 1994;14:271–305.
[7] Tanaka H, Kimura T. ACAT inhibitors in development. Exp Opin Invest Drugs 1994;3:427–36.
[8] Suckling KE, Stange EF. Role of acyl-CoA: cholesterol acyltransferase in cellular cholesterol metabolism. J Lipid Res 1985;26:647–71.
[9] Bell FP. Arterial cholesterol esterification by acyl CoAcholesterol acyltransferase: its possible significance in atherogenesis and its inhibition by drugs. In: Fears R, Levy RI, Shepard J, Packard CJ, Miller NE, editors. Pharmacological control of hyperlipidaemia. Spain: J.R. Prous Science Publishers; 1986. p. 409–22.
[10] Sliskovic DR, White AD. Therapeutic potential of ACAT inhibitors as lipid lowering and anti-atherosclerotic agents. Trends Pharmacol Sci 1991;12:194–9.
[11] Chibata I, Okumura K, Takeyama S, Kotera K. Lentinacin: a new hypocholesterolemic substance in Lentinus edodes. Experientia 1969;25:1237–8.
[12] Rokujo T, Kikuchi H, Tensho A, Tsukitani Y, Takenawa T, Yoshida K, et al. Lentysine: a new hypolipidemic agent from a mushroom. Life Sci 1970;9:379–85.
[13] Okumura K, Matsumoto K, Fukamizu M, Yasuo H, Taguchi Y, Sugihara Y, et al. Synthesis and hypocholesterolemic activities of eritadenine derivatives. J Med Chem 1974;17:846–55.
[14] Schanche JS, Schanche T, Ueland PM, Holy A, Votruba I. The effect of aliphatic adenine analogues on S-adenosylhomocysteine and S-adenosylhomocysteine hydrolase in intact rat hepatocytes. Mol Pharmacol 1984;26:553–8.
[15] Marec F, Gelbic I. High recombinagenic activities of three antiviral agents, adenine derivatives, in the *Drosophila* wing spot test. Mutat Res 1994;311:305–17.
[16] Nemec V, Slama K. Inhibition of phosphatase by open-chain nucleoside analogues in insects. Experientia 1989;45:148–50.
[17] Huang Y, Komoto J, Takata Y, Powell DR, Gomi T, Ogawa H, et al. Inhibition of S-adenosylhomocysteine hydrolase by ''acyclic sugar'' adenosine analogue D-eritadenine: crystal structure of S-adenosylhomocysteine hydrolase complexed with D-eritadenine. J Biol Chem 2002;277:7477–82.
[18] Costanzi S, Lambertucci C, Volpini R, Vittori S, Lupidi G, Cristalli G. 3′-Deoxyribofuranose derivatives of 1-deaza and 3-deaza-adenosine and their activity as adenosine deaminase inhibitors. Nucleos Nucleot Nucl Acids 2001;20:1037–41.
[19] Verseés W, Decanniere K, Pelleé R, Depoorter J, Brosens E, Parkin DW, et al. Structure and function of a novel purine specific nucleoside hydrolase from *Trypanosoma vivax*. J Mol Biol 2001;307:1363–79.
[20] Rousseau RJ, Robins RK. Synthesis of various chloroimidazo[4,5-c] pyridines and related derivatives (1). J Heterocycl Chem 1965;2:196–201.
[21] De Roos KB, Salemink CA. Deazapurine derivatives. V. New synthesis of 1- and 3-deaza-adenine and related compounds. Rec Trav Chim Pays-Bas 1969;88:1263–74.
[22] Okumura K, Oine T, Yamada Y, Tomie M, Adachi T, Nagura T, et al. Synthetic studies on eritadenine. I. Reactions of some purines with the 2,3-O-protected dihydroxybutyrolactone. J Org Chem 1971;36:1573–9.
[23] Dvorakova H, Holy A, Votruba I, Masojidkova M. Synthesis and biological effects of acyclic analogs of deazapurine nucleosides. Collect Czech Chem Commun 1993;58:629–48.
[24] Gomi T, Date T, Ogawa H, Fujioka M, Aksamit RR, Backlund PS, et al. Expression of rat liver S-adenosylhomocysteinase cDNA in *Escherichia coli* and mutagenesis at the putative NAD binding site. J Biol Chem 1989;264:16138–42.
[25] Fujioka M, Takata Y. S-Adenosylhomocysteine hydrolase from rat liver. Purification and some properties. J Biol Chem 1981;256:1631–5.
[26] American Institute of Nutrition. Report of the American Institute of Nutrition ad hoc committee on standards for nutritional studies. J Nutr 1977;107:1340–48.
[27] Otwinowski Z, Minor W. Processing of X-ray diffraction data collected in oscillation mode. Methods Enzymol 1997;276:307–26.
[28] Brünger AT, Adams PD, Clore GM, DeLano WL, Gros P, Grosse-Kunstleve RW, et al. Crystallography & NMR system: a new software suite for macromolecular structure determination. Acta Crystallogr D 1998;54:905–21.
[29] Laskowski RA, MacArthur MW, Moss DS, Thornton JM. ROCHECK: a program to check the stereochemical quality of protein structures. J Appl Cryst 1993;26:283–91.
[30] Hu Y, Komoto J, Huang Y, Gomi T, Ogawa H, Takata Y, et al. Crystal structure of S-adenosylhomocysteine hydrolase from rat liver. Biochemistry 1999;38:8323–33.
[31] Komoto J, Huang Y, Gomi T, Ogawa H, Takata Y, Fujioka M, et al. Effects of site-directed mutagenesis on the structure of S-adenosylhomocysteine hydrolase: crystal structure of D244E Mutant enzyme. J Biol Chem 2000;275:32147–56.
[32] Yamada T, Takata Y, Komoto J, Gomi T, Ogawa H, Fujioka M, et al. Catalytic mechanism of S-adenosylhomocysteine hydrolase: roles of His 54, Asp130, Glu155, Lys185, and Asp189. Int J Biochem Cell Biol 2005;37:2417–35.
[33] Steereand JA, Honek JF. Synthesis and biological activity of novel S-adenosyl-L-homocysteine hydrolase inhibitors. Bioorg Med Chem 2003;11:3229–36.
[34] Gomi T, Takata Y, Date T, Fujioka M, Aksamit RR, Backlund Jr PS, et al. Site-directed mutagenesis of rat liver S-adenosylhomocysteinase. Effect of conversion of aspartic acid 244 to glutamic acid on coenzyme binding. J Biol Chem 1990;265:16102–7.
[35] Wilson DK, Quiocho FA. A pre-transition-state mimic of an enzyme: X-ray structure of adenosine deaminase with bound 1-deazaadenosine and zinc-activated water. Biochemistry 1993;32:1689–94.
[36] Gordon RK, Ginalsk K, Rudnicki WR, Rychlewski L, Pankaskie MC, Bujnicki JM, et al. Anti-HIV-1 activity of 3-deaza-adenosine analogs inhibition of S-adenosylhomocysteine hydrolase and nucleotide congeners. Eur J Biochem 2003;270:3507–17.
[37] Yang X, Hu Y, Yin DH, Turner MA, Wang M, Borchardt RT, et al. Catalytic strategy of S-adenosyl-L-homocysteine hydrolase: transition-state stabilization and the avoidance of abortive reactions. Biochemistry 2003;42:1900–9.
[38] Shimada Y, Morita X, Sugiyama K. Eritadenine-induced alterations of plasma lipoprotein lipid concentrations and phosphatidylcholine molecular species profile in rats fed cholesterol-free and cholesterol-enriched diets. Biosci Biotechnol Biochem 2003;67:996–1006.
[39] Duncan DB. Multiple range tests for correlated and heteroscedastic means. Biometrics 1957;13:164–76.